Nonmonotonic Energy Dissipation in Microfluidic Resonators

Thomas P. Burg,[1,*] John E. Sader,[2] and Scott R. Manalis[1,3,†]

[1]*Department of Biological Engineering, Massachusetts Institute of Technology, Cambridge, Massachusetts 02139, USA*
[2]*Department of Mathematics and Statistics, The University of Melbourne, Victoria 3010, Australia*
[3]*Department of Mechanical Engineering, Massachusetts Institute of Technology, Cambridge, Massachusetts 02139, USA*

Nanomechanical resonators enable a range of precision measurements in air or vacuum, but strong viscous damping makes applications in liquid challenging. Recent experiments have shown that fluid damping is greatly reduced in fluidic embedded-channel microcantilevers. Here we report the discovery of nonmonotonic energy dissipation due to the fluid in such devices, which leads to the intriguing prospect of enhancing the quality factor upon miniaturization. These observations elucidate the physical mechanisms of energy dissipation in embedded-channel resonators and thus provide the basis for numerous applications in nanoscience and biology.

PACS numbers: 87.85.Qr, 81.07.−b, 85.85.+j

Micro- and nanomechanical cantilevers are widely used as sensitive probes for physical measurements in materials science, engineering and biology. In vacuum and air, detecting shifts in the resonance frequency enables exquisitely sensitive measurements of mass and detection of single DNA molecules, single viral particles, and single bacterial cells [1–4]. However, numerous applications in nanotechnology and the life sciences require samples to be contained in liquid. This is challenging because strong viscous damping severely degrades frequency resolution by lowering the quality factor (inverse scaled energy dissipation, Q) to around unity [5–8], in stark contrast to $Q \sim 10^4$–10^6 achieved with resonators in vacuum. In gases, miniaturizing the resonator to dimensions comparable to the mean free path provides substantial improvements [5]. However, liquids do not admit an analogous approach, and uniformly reducing the resonator size, or equivalently, increasing viscosity always lead to a monotonic degradation in Q [6].

Recently, measurements have demonstrated that viscous damping is substantially reduced by confining the (liquid) sample to a microfluidic channel embedded inside a cantilever beam surrounded by vacuum; Fig. 1(a) [9]. Such devices enable mass measurements of nanoparticles, single bacterial cells, and submonolayers of adsorbed proteins with femtogram sensitivity in liquid [9]. Applications also include ultralow volume universal detection for liquid chromatography [10], the measurement of fluid density [11–13], and the measurement of mass flow [14].

A key outstanding question is how energy dissipation, and hence sensitivity, scales with the size of the resonator and the density and viscosity of the fluid. We investigate the effect of the fluid only; variations in the intrinsic quality factor with size have been investigated elsewhere [15]. This is of particular interest since two of the most intriguing size regimes for these devices remain to be explored: (i) where the resonators are small enough to acquire mass spectra of viruses, protein complexes, and ultimately single

molecules directly in solution, and (ii) where the channel is large enough to measure the growth of mammalian cells by monitoring their mass with high precision.

In this Letter, we address this question through theory and through measurements; our results reveal surprising connections between the fluid properties, energy dissipation, and the device dimensions in liquid-filled microcantilevers. While the quality factor of conventional cantilever sensors submersed in fluid always degrades with increasing viscosity, we show that damping in liquid-filled cantilevers can increase or decrease as viscosity is increased. The physical mechanisms behind this finding are explored.

Using electrostatic actuation and an optical lever setup to measure the cantilever response, we conducted experiments with devices of 3 μm and 8 μm channel depths, see Fig. 1. The temperature of the chip was controlled at 20 °C
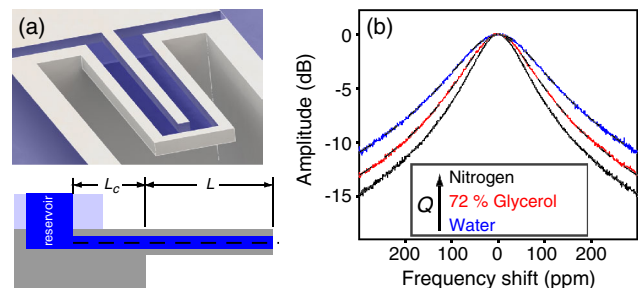

FIG. 1 (color online).   (a) Cut-away view (top) and schematic (bottom) of fluid-filled cantilever resonator surrounded by vacuum; fluid channel (blue) is completely filled. Experiments were conducted with two device types: (i) channel depth $h_{\text{fluid}} = 3.0 \pm 0.3$ μm; cantilever thickness $h_{\text{cant}} = 7.0 \pm 1.5$ μm; (ii) $h_{\text{fluid}} = 8.0 \pm 0.6$ μm, $h_{\text{cant}} = 12.0 \pm 1.5$ μm. Planar dimensions (i) and (ii): channel width $1/2 b_{\text{fluid}} = 8.0 \pm 0.25$ μm, cantilever width $b_{\text{cant}} = 33.0 \pm 0.25$ μm; $L = 210.0 \pm 0.5$ μm, $L_c = 207.5 \pm 0.25$ μm. Resonance frequency (empty): (i) 212.5 kHz, (ii) 426.8 kHz. (b) Frequency response for $h_{\text{fluid}} = 8$ μm, showing fits to damped harmonic oscillator response.

[16]. The frequency response was fitted to the model of a damped harmonic oscillator with the quality factor, resonance frequency, and response amplitude as parameters. The fit agrees with the observed frequency response to within the statistical measurement error, Fig. 1(b).

We now examine the effect of changing the fluid viscosity in these devices. A quality factor of 9172 ± 15 [17] were measured for the 8 μm channel cantilever that is surrounded by vacuum and filled with nitrogen gas. Upon filling the device with pure water, this value dropped to 5653 ± 11. However, when water was replaced with an aqueous solution of 72% glycerol by mass, the quality factor Q unexpectedly increased to 7371 ± 12; damping therefore is reduced despite a 30-fold increase in fluid viscosity; see Fig. 1(b). At the same time, shifts in the inverse square of the resonance frequency are directly proportional to changes in fluid density, i.e., $\Delta(f^{-2}) \propto \Delta\rho_{\mathrm{fluid}}$, as expected for completely filled channels.

Plotting the measured quality factor as a function of fluid viscosity reveals alternating regimes of increasing and decreasing dissipation; see Fig. 2. Initial filling with pure water lowers the quality factor of the 8 μm channel by approximately 40% (squares), but Q only degrades slightly as pure water (1 mPa s) is replaced with solutions up to 24% glycerol (2 mPa s). Between 2 mPa s and 5 mPa s, the quality factor goes through a minimum, and then improves with increasing viscosity over a range of more than one decade before starting to drop near 385 mPa s (92% glycerol). This surprising nonmonotonic dependence of damping on fluid viscosity is also observed in devices with 3 μm channels (triangles in Fig. 2). The behavior is, however, quantitatively different. While these thinner channels are damped less strongly than the deeper channels after filling with pure water, adding even small amounts of glycerol lowers the quality factor significantly. This trend reverses twice, first at 28 mPa s (72% glycerol), and again at 60 mPa s (80% glycerol).

Cantilevers with embedded fluidic channels are damped substantially less than solid cantilevers immersed in fluid, see Fig. 2. In air, the quality factor of solid cantilevers rarely exceeds a few thousand. For devices of the same dimensions used here, Q would drop to ~ 10 in water and decrease monotonically for increasing viscosity [6].

The physical mechanisms which cause the observed nonmonotonic dependence of damping on viscosity are now explored using a leading-order theoretical model that provides a self-consistent treatment of the fluid and solid mechanics; this is achieved by combining the Navier-Stokes equations with Euler-Bernoulli beam theory. The measured quality factor is decomposed into the intrinsic quality factor Q_{int} and the quality factor due to the fluid Q_{fluid}, as $Q^{-1} = Q_{\mathrm{int}}^{-1} + Q_{\mathrm{fluid}}^{-1}$ [15]. To calculate Q_{fluid}, we determined the flow generated in the channel by solving the Navier-Stokes equation for the boundary conditions imposed by the moving solid, assuming the vibration amplitude is small [6].
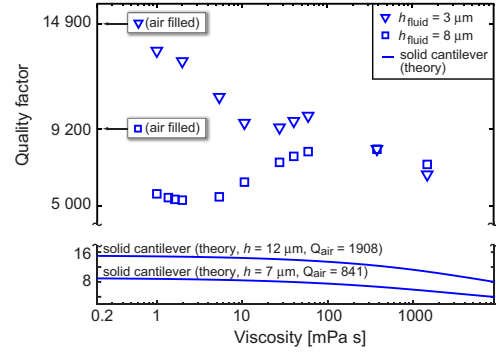

FIG. 2 (color online). Quality factor of vacuum encapsulated cantilevers with 3 and 8 μm channels as a function of fluid viscosity. Viscosity was varied by injecting different solutions of glycerol in water. Solid lines show the predicted quality factor [6] for solid cantilevers that have the same outer dimensions as the embedded-channel cantilevers used here.

The local displacement field in a short section of the beam corresponds to a rigid-body rotation and translation, as described by Euler-Bernoulli beam theory. In its simplest configuration, the channel inside the cantilever is precisely centered about the beam neutral axis. Dissipation is then, to leading order, caused by shearing of the fluid due to the effects of inertia. The magnitude of this effect is governed by the dimensionless frequency $\beta = (h_{\mathrm{fluid}}/\delta)^2$ [18], where h_{fluid} is the channel height and $\delta = \sqrt{\mu/(\rho_{\mathrm{fluid}}\omega)}$ is the Stokes length, μ is the shear viscosity, ρ_{fluid} is the fluid density and ω the radial frequency of oscillation. The quality factor due to the fluid is given by $Q_{\mathrm{fluid}} = 2\pi E_{\mathrm{stored}}/E_{\mathrm{diss}}$, where E_{stored} is the energy stored in the resonator and E_{diss} is the energy dissipated per cycle. The stored energy is $E_{\mathrm{stored}} = 1/2 kA^2 \sim \omega^2 \rho_{\mathrm{cant}} h_{\mathrm{cant}} b_{\mathrm{cant}} L A^2$, with ρ_{cant} denoting the weighted average mass density of the solid and liquid volume, k the dynamic spring constant and A is the oscillation amplitude. From the rate of energy dissipation per unit volume, $2\mu\mathbf{e}:\mathbf{e}$, where $\mathbf{e}$ is the rate-of-strain tensor, we obtain the scaling relation $E_{\mathrm{diss}} \sim \mu\omega A^2 h_{\mathrm{fluid}} b_{\mathrm{fluid}}/L$. This analysis then gives

$$Q_{\mathrm{fluid}} = F(\beta)\frac{\rho_{\mathrm{cant}}}{\rho_{\mathrm{fluid}}}\left(\frac{h_{\mathrm{cant}}}{h_{\mathrm{fluid}}}\right)\left(\frac{b_{\mathrm{cant}}}{b_{\mathrm{fluid}}}\right)\left(\frac{L}{h_{\mathrm{fluid}}}\right)^2, \quad (1)$$

where the dimensionless function $F(\beta)$ is

$$F(\beta) = 0.0538\beta\left(\int_{-1/2}^{1/2}\left|1 - \frac{1-i}{2}\right.\right.$$

$$\left.\left.\times\sqrt{\frac{\beta}{2}}\frac{\cosh((1-i)\sqrt{\frac{\beta}{2}}s)}{\sinh((1-i)\sqrt{\frac{\beta}{2}})}\right|^2 ds\right)^{-1}, \quad (2)$$

and is well approximated by $F(\beta) \approx 0.152\sqrt{\beta} + 38.7/\beta$; this formula exhibits a maximum error of 13% for all β. Equation (2) reveals a minimum at $\beta \approx 46$, which coincides approximately with the observed minimum in Q between 2 mPa s and 5 mPa s in the 8 μm device; see

Fig. 2. This point marks the transition between different fluid flow regimes, which we now explore.

In the limit of *high inertia* ($\beta \gg \beta_{\min}$), fluid vorticity generated at the channel wall diffuses only a small distance into the channel. Outside this (thin) viscous boundary layer, flow is dominated by inertia (i.e., inviscid flow) and is 180° out-of-phase with the beam displacement, see Fig. 3 ($\beta = 1000$). As such, to match the no-slip condition, flow in the immediate vicinity of the wall must be given by Stokes' second problem for the planar oscillations of an infinite wall [19]. Therefore, damping increases as $\sqrt{\mu}$, giving the leading-order asymptotic dependence $F(\beta) \sim \sqrt{\beta}$, as above. This trend is confirmed in measurements with the 8 μm device where it is observed that after filling with water ($\beta \sim 159$), the quality factor drops substantially with increasing viscosity, and continues to decrease in the range $1 < \mu < 2$ mPa s.

For *low inertia* ($\beta \ll \beta_{\min}$), the viscous boundary layers at the top and bottom walls overlap and dominate the flow field. Since there is little inertia, the fluid now tracks the solid displacement and closely resembles a rigid-body translation and rotation, as shown in Fig. 3. At $\beta = 10$, the residual axial velocity after subtracting rigid-body rotation and translation of the beam is small, and lags the solid velocity by approximately 90°. The total rate-of-strain decreases with increasing viscosity, and the net energy dissipation scales as μ^{-1}. This explains the unexpected improvement in Q with increasing viscosity found in the 8 μm device for $5 < \mu < 100$ mPa s.

At higher viscosities ($\mu > 100$ mPa s), the above model fails to predict the observed decrease in quality factor of the 8 μm device with increasing viscosity. Increased damping at high viscosity may be explained by a small asymmetry of the embedded channel cantilever about its midplane (neutral axis) due to finite fabrication tolerances. Based on the precision of individual fabrication steps, an off-axis placement, z_0, of the channel of ~ 0.5 μm is expected. This leads to significant axial extension and compression of the fluid channel under cantilever bending,

causing fluid to stream into and out of the cantilever from the reservoir; see Fig. 1(a).

In the high inertia regime ($\beta > \beta_{\min}$), energy loss through this pumping mechanism is significantly smaller than that due to inertial shearing of the fluid inside the cantilever, as above. This contrasts to low-inertia flows ($\beta < \beta_{\min}$), where viscous losses induced by pumping are significant. In this regime of small β,

$$F(\beta) \approx \frac{38.7\beta}{\beta^2 + 564(\frac{z_0}{h_{\text{fluid}}})^2(1 + \frac{\beta^2}{8400})}, \quad (3)$$

yielding $F(\beta) \sim \beta$ as $\beta \to 0$; see Fig. 4 (dash-dotted). This off-axis effect is dominant in measurements with the 3 μm device where, owing to the low channel height, all values of β are much smaller than $\beta_{\min}$. Although the precise placement away from the neutral axis is not known, Fig. 4 shows good agreement between theory and experiment in the range $\beta > 1$ for values of z_0 well within fabrication tolerances. The quantitative differences between the model and measurements for the 8 μm channel, which possesses a square cross section, are not surprising given the model is derived under the assumption of an infinitely thin fluid channel and infinitely long length relative to its width. As expected, agreement between the model and measurement is improved for the thinner 3 μm device; see Fig. 4.

Surprisingly, measurements with the 3 μm device display a minimum in Q at $\beta \sim 1$, followed by a maximum around $\beta \sim 0.1$. At the same time, the total quality factor decreases only by a factor of 2 for a 1500-fold increase in viscosity. Such unusual behavior can be explained by the significant effects of fluid compressibility for $\beta < 1$. Damping is reduced in this regime, because the fluid partially accommodates the change in volume of the embedded fluidic channel by elastic expansion and compression, reducing the volumetric flux into the channel. This results in smaller shear velocity gradients and a lower rate of strain. Including the effects of fluid compressibility in
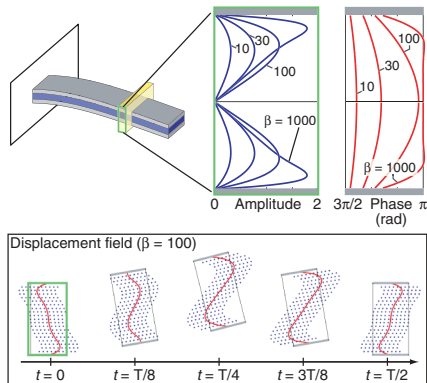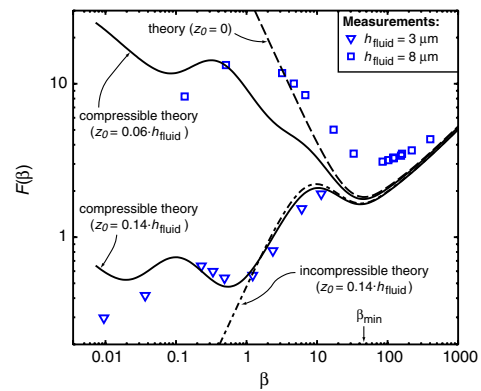

FIG. 3 (color online). (top right) Amplitude and phase of velocity in fluid channel relative to the beam. (bottom) Displacement field for $\beta = 100$ over half-period $t \in [0, T/2]$.

FIG. 4 (color online).   Measurements and model predictions of the normalized quality factor. Nonzero off-axis placement, z_0, leads to significant dissipation in the low-inertia regime ($\beta < \beta_{\min}$); velocity gradients reduced by fluid dilatation (compressible model, solid lines) in the regime $\beta < 1$.

the model predicts the occurrence of two minima in $F(\beta)$ that individually result from the effects of fluid compressibility in the cantilever and in the rigid lead channel that connects to the fluid reservoir. This compressible model is derived using the same formalism as Eqs. (1)–(3), with the constitutive equation for a compressible Newtonian fluid [19]. In essence, as viscosity increases, energy dissipation is enhanced up to a level where compressibility becomes important, following which the shear velocity gradients are reduced which decreases energy dissipation. Since flow in the cantilever differs from that in the lead channel, two maxima in energy dissipation result in β-space, and hence two minima in the quality factor. Calculations show a minimum at $\beta \sim 1$ (due to the lead channel) and a maximum at $\beta \sim 0.1$ (due to competition between the lead channel and the cantilever), consistent with our measurements. For $\beta \ll 0.1$, the effects of compressibility are so great that the volumetric flux into the channel is minimal, and this results in an increase in quality factor with increasing viscosity. It is important to note that higher order effects, such as curvature, shear deformation and end effects in the system (all of equal order) are expected to ultimately limit the quality factor at very high viscosity. These may be at least partially responsible for the observed decreasing trends in Q at and below $\beta \sim 0.1$.

Finally, we examine how device size affects the quality factor. In β-space, measurements at high viscosity may also be interpreted in terms of an equivalent reduction in the size of embedded-channel cantilevers at fixed low viscosity. Our results then point towards the possibility of maintaining very high quality factors as device dimensions are reduced by up to 2 orders of magnitude, see Fig. 4. For example, scaling down the 8 μm cantilever 30-fold in length, width, and thickness would improve sensitivity by more than 4 orders of magnitude, while the concomitant change in β from ~ 159 to ~ 5 for water should cause viscous damping to decrease. This would yield a mass resolution of ~ 0.1–1 attograms [20], enabling the direct, solution-based measurement of mass and mass density of nanoscopic particles, such as viruses and quantum dots. If the readout can be improved to be solely limited by thermomechanical noise of the resonator [21], it is conceivable that single-molecule sensitivity can be attained. This could provide a unique alternative to dynamic light scattering for analyzing polydisperse macromolecular samples, such as neurotoxic amyloid oligomers.

Devices with large channel heights of 10–100 μm operating in the large-β regime are of great interest for mass and density based flow cytometry of mammalian cells. If the channel walls are thin compared to h_{fluid}, the on-axis model in Eq. (1) predicts $Q_{\text{fluid}} \propto L/\sqrt{h_{\text{fluid}}}$; thus, for linear scaling in all dimensions, Q_{fluid} is expected to improve with the square root of the scale factor. Based on a frequency resolution in the parts-per-billion range in a 1 Hz bandwidth, as previously demonstrated [9], mass measurements of cells (~ 1–10 ng) with a precision of one part in 10^4 or better could then be feasible. Such measurements could be

used to investigate subtle effect of drugs on cell growth at the single-cell level, which would provide valuable information in, for example, the development of new agents for cancer treatment.

A unique aspect of suspended micro- and nanochannel resonators is their sensitivity to the finite compressibility of the sample. Appropriately designed resonators may allow the pumping mechanism to be amplified, generating negative pressures sufficient to cause cavitation. The dependence of damping on compressibility could also enable high-throughput stiffness-based flow cytometry, which might be a valuable tool for the label-free recognition of diseased cells in populations of healthy cells [22].

*Present address: Max-Planck-Institute for Biophysical Chemistry, 37077 Goettingen, Germany.
†scottm@media.mit.edu
[1] Y. T. Yang *et al.*, Nano Lett. **6**, 583 (2006).
[2] A. Gupta, D. Akin, and R. Bashir, J. Vac. Sci. Technol. B **22**, 2785 (2004).
[3] A. Gupta, D. Akin, and R. Bashir, Appl. Phys. Lett. **84**, 1976 (2004).
[4] B. Ilic *et al.*, Nano Lett. **5**, 925 (2005).
[5] M. Li, H. X. Tang, and M. L. Roukes, Nature Nanotech. **2**, 114 (2007).
[6] J. E. Sader, J. Appl. Phys. **84**, 64 (1998).
[7] T. Braun *et al.*, Phys. Rev. E **72**, 031907 (2005).
[8] H. Zhang *et al.*, J. Micromech. Microeng. **15**, 1911 (2005).
[9] T. P. Burg *et al.*, Nature (London) **446**, 1066 (2007).
[10] S. Son *et al.*, Anal. Chem. **80**, 4757 (2008).
[11] P. Enoksson, G. Stemme, and E. Stemme, Sens. Actuators A, Phys. **54**, 558 (1996).
[12] D. Westberg *et al.*, J. Micromech. Microeng. **7**, 253 (1997).
[13] D. Sparks *et al.*, Lab Chip **3**, 19 (2003).
[14] P. Enoksson, G. Stemme, and E. Stemme, J. Microelectromech. Syst. **6**, 119 (1997).
[15] K. Y. Yasumura *et al.*, J. Microelectromech. Syst. **9**, 117 (2000).
[16] Isothermal conditions exist as demonstrated by amplitude independent quality factor; a scaling analysis reveals a maximum temperature differential $\lesssim 10^{-4}\,^\circ$C over the cantilever length.
[17] SD of 10 consecutive measurements without fluid change; ± 75 uncertainty from 17 repeated fill and dry cycles.
[18] This parameter is often referred to under different names, e.g., Reynolds, inverse Stokes or Womersley number.
[19] G. K. Batchelor, *An Introduction to Fluid Dynamics* (Cambridge University Press, Cambridge, England, 1974).
[20] The quality factor is assumed to be limited by the fluid; for cantilevers of submicron thickness, $Q_{\text{int}} \gg 10\,000$ have been demonstrated [15].
[21] K. L. Ekinci, Y. T. Yang, and M. L. Roukes, J. Appl. Phys. **95**, 2682 (2004).
[22] S. E. Cross *et al.*, Nature Nanotech. **2**, 780 (2007).